The Report Committee for Mathilde Michèle Luycx
Certifies that this is the approved version of the following report:

Tool Design, Physics and Interpretation of Neutron-Gamma Density

APPROVED BY
SUPERVISING COMMITTEE:

Carlos Torres-Verdín, Supervisor

Erich Schneider

Tool design, Physics and Interpretation of Neutron-Gamma density

by

Mathilde Michèle Luycx

Report

Presented to the Faculty of the Graduate School of

The University of Texas at Austin

in Partial Fulfillment

of the Requirements

for the Degree of

Master of Science in Engineering

The University of Texas at Austin

Mai 2016

Acknowledgements

I would like to express my sincere gratitude to my adviser, Dr. Carlos Torres-Verdín for the opportunity to be part of his group, for his excellent guidance, advice and support. I would like to thank Dr. Erich Schneider for serving on my committee and for his guidance in nuclear physics. I would like to thank Schlumberger Doll Research for a great internship and Jeffrey Miles for his mentorship and for sharing his knowledge on nuclear physics and nuclear modeling. I am also grateful to John Rasmus and Cornelis Huiszoon for making the opportunity of an internship at Schlumberger possible. I am thankful to Reynaldo Casanova, Roger Terzian and Frankie Hart for their administrative support and to Nigel Quayle for helping me join this program.

Thanks to my friends and colleagues in the group for their help and suggestions and to my family for their love and support.

The work reported in this report was funded by The University of Texas at Austin's Research Consortium on Formation Evaluation, jointly sponsored by Anadarko, Aramco, Baker-Hughes, BHP Billiton, BP, China Oilfield Services LTD., ConocoPhillips, Det Norske, ENI, ExxonMobil, Hess, Paradigm, Petrobras, Repsol, DEA, Schlumberger, Shell, Statoil, TOTAL, Wintershall and Woodside Petroleum Limited.

Abstract

Tool design, Physics and Interpretation of Neutron-Gamma density

Mathilde Michèle Luycx, M.S.E.

The University of Texas at Austin, 2016

Supervisor: Carlos Torres-Verdín

Chemical radioactive sources pose health, safety, and environmental risks. Pulsed neutron generators have replaced Americium/Beryllium sources for the measurement of neutron porosity. However, Cesium 137 (Cs-137) is still mainly used to measure bulk density. Neutron-Gamma density is a new radioisotope-free measurement of density based on neutron-induced inelastic gamma rays.

The first part of this report reviews relevant literature to the Neutron-Gamma density measurement and to the modeling of nuclear logging tools. The second part of this report investigates the nuclear physics behind Neutron-Gamma density and presents the development of a tool design optimized for the measurement. The third part of this report regards the development of a real-time interpretation algorithm. The objective of the algorithm is to correct for the changes in spatial distribution and source strength of the neutron-induced gamma ray source. These source variations are caused by fast neutron transport. Therefore, the interpretation algorithm has inputs of fast neutron and

gamma ray counts. We achieve an accuracy of 0.019 g/cm^3 in clean formation and 0.034 g/cm^3 in shale and shaly formations. In the last part of this report, we study some of the measurement limitations regarding the density range and the influence of standoff. The algorithm does not accurately estimate higher densities (densities greater than 2.89 g/cm^3) and standoff should be kept to a maximum of 0.25 inch for light mud. Finally, the depth of investigation of Neutron-Gamma Density is twice the depth of investigation of Gamma-Gamma Density. This work is presented as part of the PhD fast track option and will be extended to a PhD dissertation in the future.

Table of Contents

List of Figures

Chapter 1: Introduction

Density measurements are traditionally performed using a Cs-137 radioactive source that generates 662 keV gamma rays. Gamma rays are attenuated in the formation. Their attenuation almost solely depends on formation density; therefore gamma counts are used to estimate the density of the formation. The oil industry is interested in mitigating the security, health, and environmental risks associated with the use of radioactive sources, such as Cs-137. Neutron-Gamma density has been developed as a radioisotope-free alternative to the traditional Gamma-Gamma density measurement. Neutron-Gamma density uses a pulse-neutron generator that emits high energy neutrons. The formation nuclei become excited by high energy neutrons and emit gamma rays upon de-excitation. Neutron-induced gamma rays are attenuated in a similar manner as the Gamma-Gamma density measurement. Therefore, Neutron-Gamma density counts hold information about formation density. The challenge of the Neutron-Gamma density measurement is to decouple the influence of neutron transport from the influence of Compton scattering that is dominated by bulk density. Understanding and correcting for the influence of fast neutron transport over the total counts is crucial to evaluate bulk density.

Moreover, the development of fast forward modeling associated with inversion techniques would improve the measurement interpretation in formations where the correction of fast neutron transport is deficient as well as in complex 3D geometry such as deviated wells, invaded formations, and thinly laminated formations.

Chapter 2: Literature Review

In this section, I review literature relevant to the development of the Neutron-Gamma density real-time interpretation algorithm.

2.1 Modeling of Nuclear Logging Tools

Neutron-Gamma density involves multiple and complex nuclear interactions. Since this work is purely based on numerical simulations, accurate modeling of neutron and gamma ray counts is crucial. The transport of nuclear particles is described by the Boltzmann transport equation

$$\frac{1}{v(E)}\frac{\partial \boldsymbol{\psi}}{\partial t} = -\Sigma_t \boldsymbol{\psi} - \nabla \bullet \boldsymbol{\psi}\hat{\boldsymbol{\Omega}} + \int_0^{\infty} dE' \int_{4\pi} d\hat{\boldsymbol{\Omega}}' \boldsymbol{\psi}(E', \hat{\boldsymbol{\Omega}}') \left[\Sigma_s(E' \to E, \hat{\boldsymbol{\Omega}}' \bullet \hat{\boldsymbol{\Omega}}) \right] + S \tag{2.1}$$

where $\boldsymbol{\psi} = \boldsymbol{\psi}(\mathbf{r}, E, \hat{\boldsymbol{\Omega}}, t)$ is angular flux at position $\mathbf{r}$, energy E, and direction $\hat{\boldsymbol{\Omega}}$ at time t, $v(E)$ is particle velocity at energy E, Σ_t is total interaction cross section. The scattering cross section, Σ_s, represents the probability of scattering from E' and $\hat{\boldsymbol{\Omega}}'$ to E and $\hat{\boldsymbol{\Omega}}$. and $S = S(\mathbf{r}, E, \boldsymbol{\Omega}, t)$ is the source of particles at position r, energy E, and direction $\hat{\boldsymbol{\Omega}}$ at time t.

Lewis (1938) shows that nuclear transport problems can be solved deterministically using approximations to solve the Boltzmann transport equation. Tittle et al. (1961) and Bertozzi et al. (1981) investigate these methods to simulate neutron and density tool responses.

However, deterministic solutions are not adequate in 3D geometries and complex problems. Stochastic methods such as MCNP (Monte Carlo for N-particle transport, Goorley, 2014) allow for accurate modeling in complex geometries since the probability of interaction and transport of millions of particles are calculated individually to evaluate quantities by the law of large numbers. This method is computationally expensive but very accurate. Variance reduction techniques such as cutoffs or weight windowing can be used to improve efficiency (Booth et al., 1984). Moreover, fast forward modeling based on first order linear perturbation theory and sensitivity functions has been developed by Watson (1984, 1922), Case et al. (1994), Couët et al. (1993) and implemented to formation evaluation and petrophysical interpretation by Mendoza et al. (2007, 2010, 2010b).

In this work, our modeling is based on the MCNP6.1.1-Beta algorithm (Goorley, 2014). MCNP6.1.1-Beta allows for accurate modeling and benefits from a tagging feature, useful for understanding the complex physics of the measurement. This feature reveals the respective influence of annihilation, bremsstrahlung radiation, and inelastic interactions in the creation of the gamma rays used for the density measurement.

2.2 SOURCELESS MEASUREMENT OF FORMATION DENSITY

The concept of sourceless density was first introduced by Weller et al.. A description of the Neutron-Gamma density measurement and its accuracy were published in 2012 by Evans et al. and Reichel et al.

Based on a customer survey to clients of different specialties worldwide, Weller et al. found that the elimination of chemical nuclear sources was the fourth highest priority in the development of the next generation of LWD logging tools. Neutron-Gamma density was proposed as a solution to eliminate the risk involved in using

chemical sources. Reichel et al. introduced a LWD Neutron-Gamma density tool that uses neutron-induced inelastic gamma rays to measure density. When inelastic gamma rays are considered, the strength and position of the neutron-induced gamma ray source remain relatively constant with formation porosity.

Reichel et al. state that inelastic gamma ray counts are affected by two major influences: the attenuation of fast neutrons to the point of gamma ray creation and the following attenuation of inelastic gamma rays. A correction algorithm is implemented to correct inelastic gamma ray counts for fast neutron attenuation in order to determine density. Evans et al. apply additional corrections for high Sigma formations, shale, and gas-filled formations. The correction algorithm inputs and the algorithm procedure are not disclosed. The extent and exact form of the additional corrections are also not described. The formation density limitations for the algorithm are 1.7 to 2.9 g/ cm^3. The accuracy in clean formations is 0.025 g/cm^3 and 0.045 g/cm^3 in shale.

The depth of investigation of Neutron-Gamma density is found to be 25 cm, which is 2.5 times deeper than the traditional Gamma-Gamma density. Consequently, Neutron-Gamma density is less sensitive to shallow invasion and well deviation.

Reichel et al. and Evans et al. report promising results, but no paper to date has clearly stated the procedure or the required corrections to perform a radioisotope-free measurement of density.

2.3 Environmental Effects of Neutron-Gamma density

Neutron-Gamma density is subject to environmental effects. Reichel et al. describe the most significant effects as: borehole size, standoff, mud weight, and Sigma —the macroscopic thermal neutron capture cross section of the formation. The influence of Sigma and mud salinity are minimal since only inelastic gamma rays are used to

perform the measurement. Inelastic gamma rays are generated from fast neutrons that are only slightly affected by changes in formation capture cross section. Evans et al. indicate that a critical input is caliper. An enlarged borehole will shift the measured density closer to the mud density. Therefore, the influences of mud weight and borehole enlargement are correlated and the borehole size input should be as accurate as possible to perform the optimal correction.

Reichel et al. indicate using the spine and ribs technique to correct for borehole environmental effects of Neutron-Gamma density. This technique was initially developed for Gamma-Gamma density by Wahl et al. and Tittman et al. and does not require borehole size, standoff, or mud weight as inputs.

2.4 INVERSION ALGORITHM

The development of the real-time interpretation algorithm is based on empirical corrections using fast neutron counts. The correction coefficients used to correct inelastic gamma ray counts for fast neutron transport are obtained using an inversion algorithm.

Aster et al. (2005) references practical techniques to implement efficient inversion algorithms. The Levenberg-Marquardt and Occam methods are both referenced for non-linear inversion.

Chapter 3: Physics and Tool Design

In this chapter, we study the physics of the Neutron-Gamma density measurement. The physics of the measurement guides us to develop an optimal tool design and to derive a real-time interpretation algorithm of the measurement.

3.1 Physics and Nuclear Interactions

The interactions of nuclear particles leading to the measurement of Neutron-Gamma density are complex. Reichel et al. indicate that the measurement count rate is affected by three main effects: the fast neutron flux attenuation, the inelastic gamma ray production cross section and the gamma ray attenuation afterwards. Other type of particle transport and interactions contribute significantly to the measurement count rate.

High energy fast neutrons are generated by a pulsed neutron generator. These high energy neutrons undergo elastic scattering interactions and inelastic scattering interactions with the formation nuclei losing more and more energy. During inelastic scattering, the formation nuclei become excited and release inelastic gamma rays upon de-excitation. Neutrons can also loose energy and start diffusing in the formation as thermal neutrons. Thermal neutrons are captured by formation nuclei which emit capture gamma rays upon de-excitation. Both capture and inelastic gamma rays are attenuated through Compton scattering (and photoelectric absorption at lower energies).

Interactions such as Compton scattering also lead to electrons being ejected from their cloud. These free electrons can release their energy and generate bremsstrahlung photons. Additionally, inelastic gamma rays - born at higher energy - can be absorbed during pair production interactions where a positron-electron pair is created. Upon

interaction with electrons, the positrons generate annihilation photons at their birth location (the migration distance of positrons is a few millimeters).

Neutron-Gamma density uses inelastic gamma rays to limit variability in the neutron-induced gamma ray source. Inelastic gamma rays are produced by fast neutrons, which do not diffuse in the formation and are less influenced by changes in hydrogen index than thermal neutrons. Therefore, the neutron-induced gamma ray source is also less affected by changes in hydrogen index, thus limiting variations in the spatial distribution of the secondary source.

A 10 microsecond time gate is implemented to tally non-capture gamma rays at gamma ray detectors. In the first 10 microseconds after the burst, fast neutrons have not lost sufficient energy to reach energies where capture interactions dominate. The neutrons remain at high energies (above the energy threshold for inelastic interactions), and capture is thus dominated by other interactions (non-capture interactions). Non-capture gamma ray counts are used to approximate inelastic gamma ray counts.

Contributions to non-capture counts from annihilation radiation, pair production, and bremsstrahlung radiation need to be considered in the measurement. In **figure 3.1**, we present the contribution of these interactions to the detector counts.

The detected gamma rays are generated from various interactions besides inelastic scattering. However the linear attenuation with respect to density observed in **figure 3.1** indicates that these gamma rays are subsequently undergoing Compton scattering interactions. Therefore, non-capture gamma counts carry information about density despite being generated from other type of interactions. We will develop a real-time interpretation algorithm to decouple the influence of Compton scattering interactions from changes in source strength and source spatial distribution.

3.2 TOOL DESIGN

To date no papers have been published that study the most effective tool design to perform Neutron-Gamma density. The design of the tool and the choice of source-detector spacing are challenging because two opposite effects influence the optimal tool configuration. Fast neutron transport dominates the measurement until non-capture gamma rays are produced. After this point, gamma ray transport dominates.

On one hand, the distance between the neutron-induced source and the gamma detector has to be large enough to carry sufficient information about the gamma transport and display sufficient accuracy for the density measurement. On the other hand, if the detector is spaced too far from the neutron source, the detected count rates and the statistics of the measurement are reduced. The performance of Neutron-Gamma density are compared to Gamma-Gamma density in **figure 3.2**. Then, a point source was used in an infinite homogenous medium to eliminate tool effects. I compare the attenuation of gamma rays with density to evaluate the accuracy of each tool. Increasing detector spacing to improve accuracy is three times more efficient for the Gamma-Gamma density tool compared to the Neutron-Gamma density tool.

A long space detector located 90 cm from the source achieves similar accuracy to a short space Gamma-Gamma density detector and receives a number of photons within the same order of magnitude per source particle emitted. Another detector is located 50 cm from the source for the Neutron-Gamma density short space measurement. A fast neutron detector is located 25 cm from the source. The tool design includes boron carbide shielding to prevent contributions from particles that do not interact with the formation. The final tool design is presented in **figure 3.3**.

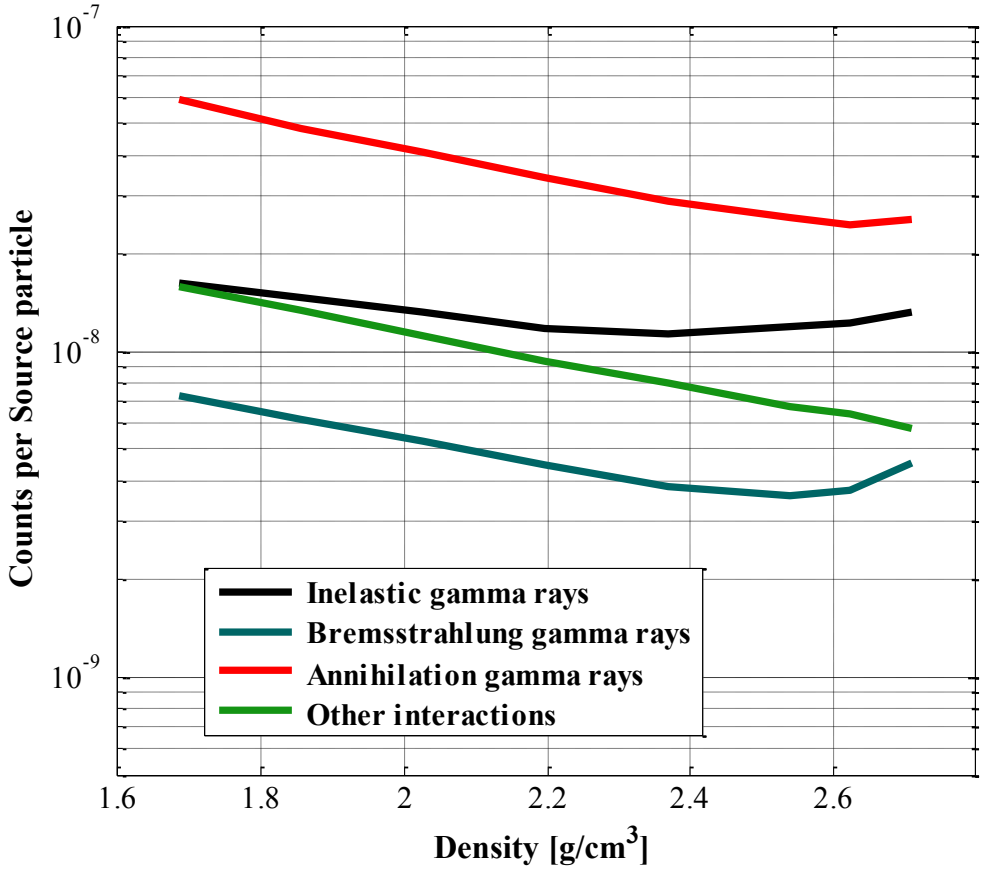

Figure 3.1: Reaction of origin of non-capture gamma rays tallied at a Neutron-Gamma density long space gamma ray detector for a 0 p.u limestone formation.

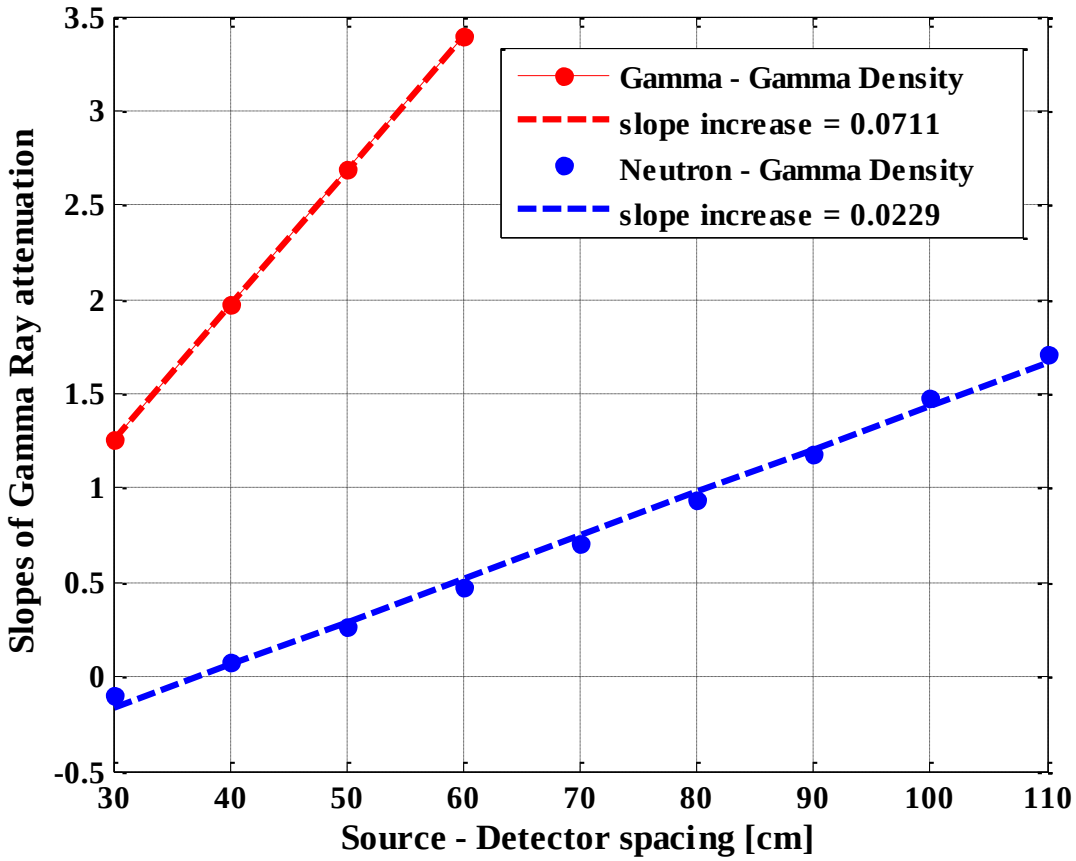

Figure 3.2: Slopes of gamma ray attenuation with density for different source-detector spacing.

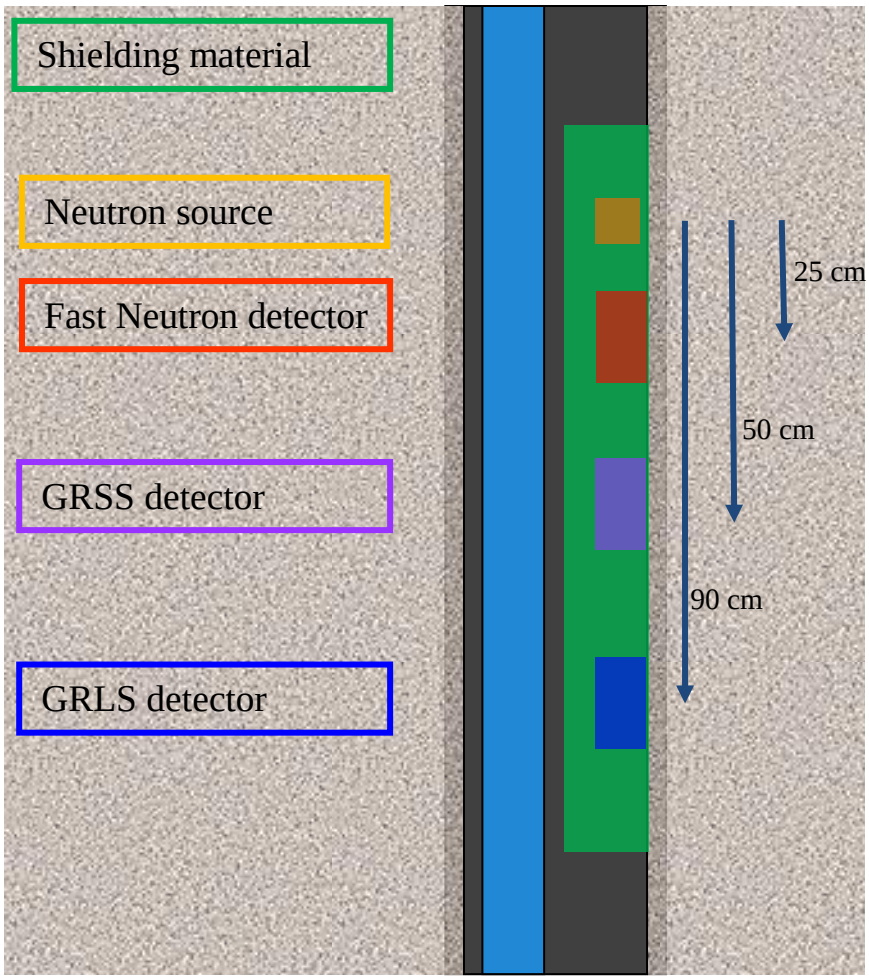

Figure 3.3: Longhorn Neutron-Gamma density tool design.

Chapter 4: Real-Time Interpretation Algorithm

I develop a real-time interpretation algorithm to correct non-capture gamma ray counts for the changes in source strength and spatial distribution of the neutron-induced gamma ray source. These changes result from the influence of fast neutron transport.

The main input of the interpretation algorithm comes from the counts at the long space gamma ray detector. Since the detector is located at 90 cm from the source, the gamma rays are more likely to undergo Compton interactions and carry more information about formation density. At different spacing, gamma counts are similarly affected by fast neutron transport and resulting variations in the neutron-induced gamma source. Performing the ratio of gamma ray counts at two different detector spacing allows us to compensate for some of the fast neutron transport influence (**figure 4.1**).

The algorithm also uses fast neutron counts from the detector located at 25 cm from the source to correct inelastic gamma ray counts for fast neutron transport. I solve the following inverse problem

$$f(GRLS/GRSS, Fast\_N) = m_1 \cdot \rho + m_2 \tag{4.1}$$

where ρ is the bulk density, and f is a function of the fast neutron counts as well as the ratio of long and short space gamma ray counts. The function f is described by

$$\begin{aligned} \log_e(\text{Corrected GR counts}) &= f(GRLS/GRSS, Fast\_N) \\ &= \log_e\left(\frac{GRLS}{GRSS}\right) - \left[\sum_{i=0}^{2} a_i \times \log_e(Fast\_N)^i\right] - \alpha \times (1 - C_{sh}) \end{aligned} \tag{4.2}$$

and represents the corrected gamma ray counts, where C_{sh} is the relative shale concentration in the matrix. I perform the Levenberg-Marquardt minimization on the error function

$$e(m_1, m_2, a_1, a_2, a_3, \alpha) = \left\| \log_e\left(\frac{GRLS}{GRSS}\right) - \left[\sum_{i=0}^{2} a_i \times \log_e(Fast\_N)^i\right] - \alpha \times (1 - C_{sh}) - (m_1 \times \rho + m_2) \right\|_2^2 \tag{4.3}$$

The inversion results are presented in **figure 4.2** for clean formations. In shale and shaly formations, a linear equation

$$\log_e(\text{Corrected MCNP counts}) = m_1(C_{sh}) \times \rho + m_2(C_{sh}) \tag{4.4}$$

is used to predict the formation bulk density according to shale concentration (**Figure 4.3**). The inversion results for shale and shaly formations are presented in **figure 4.4**. C_{sh} can be obtained through Gamma Ray or spectroscopy logging.

The accuracy of the density measurement is 0.019 g/cm^3 in clean formations and 0.034 g/cm^3 in shale and shaly formations. This accuracy is calculated by adding 5 % Gaussian noise.

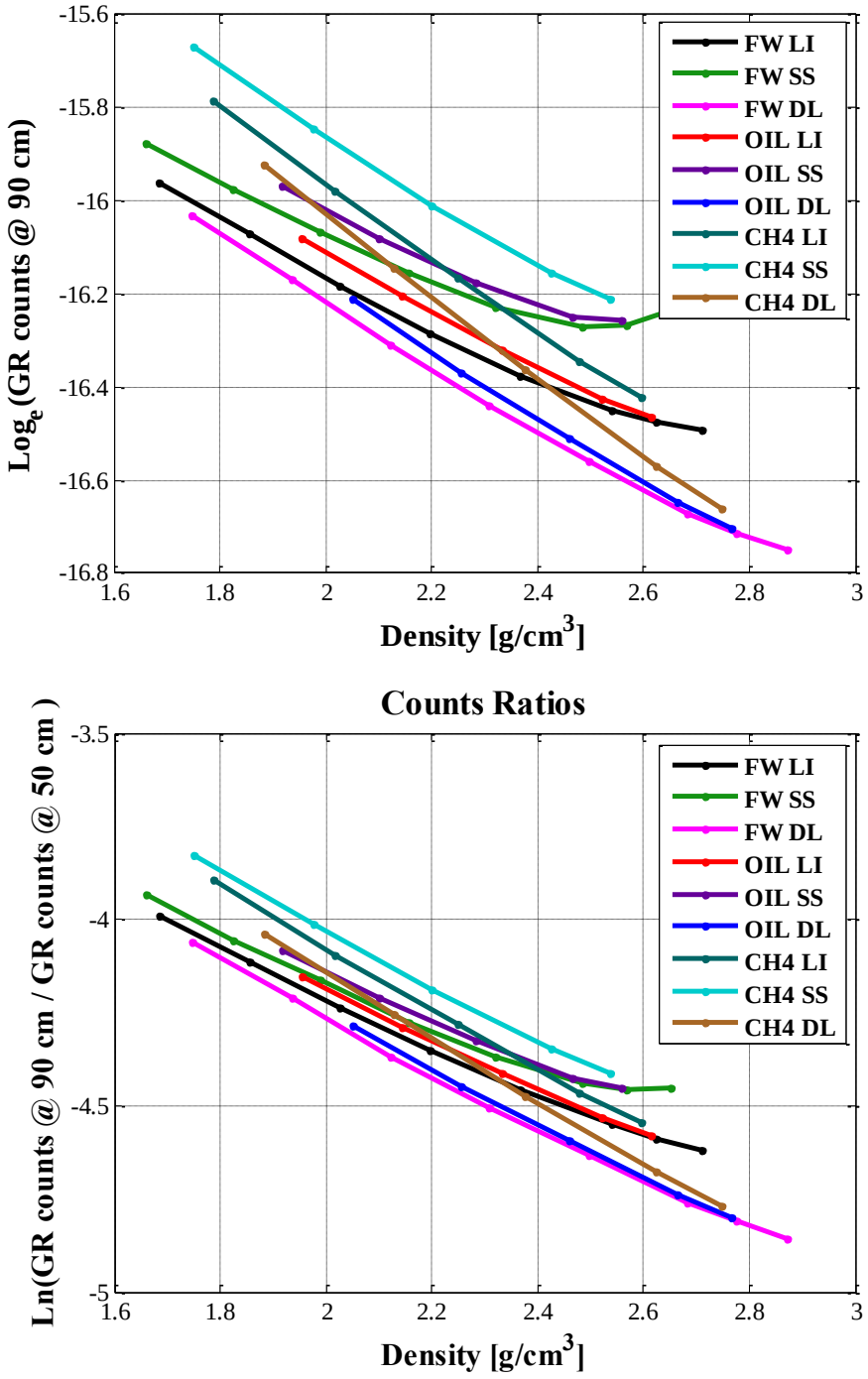

Figure 4.1: Neutron Gamma density gamma ray counts. **Top** - Gamma ray counts at the long space detector. **Bottom** - Ratio of gamma ray counts at the long space detector and short space detector.

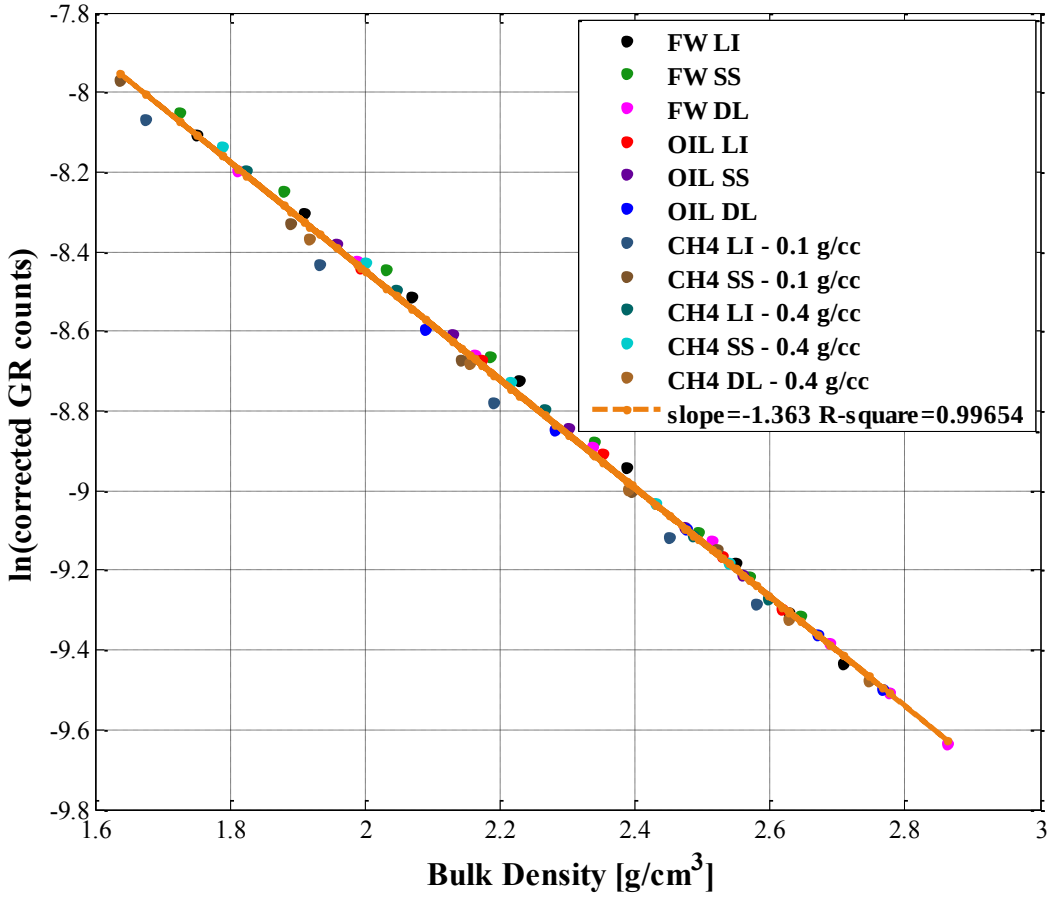

Figure 4.2: Results of the inversion algorithm for clean formations.

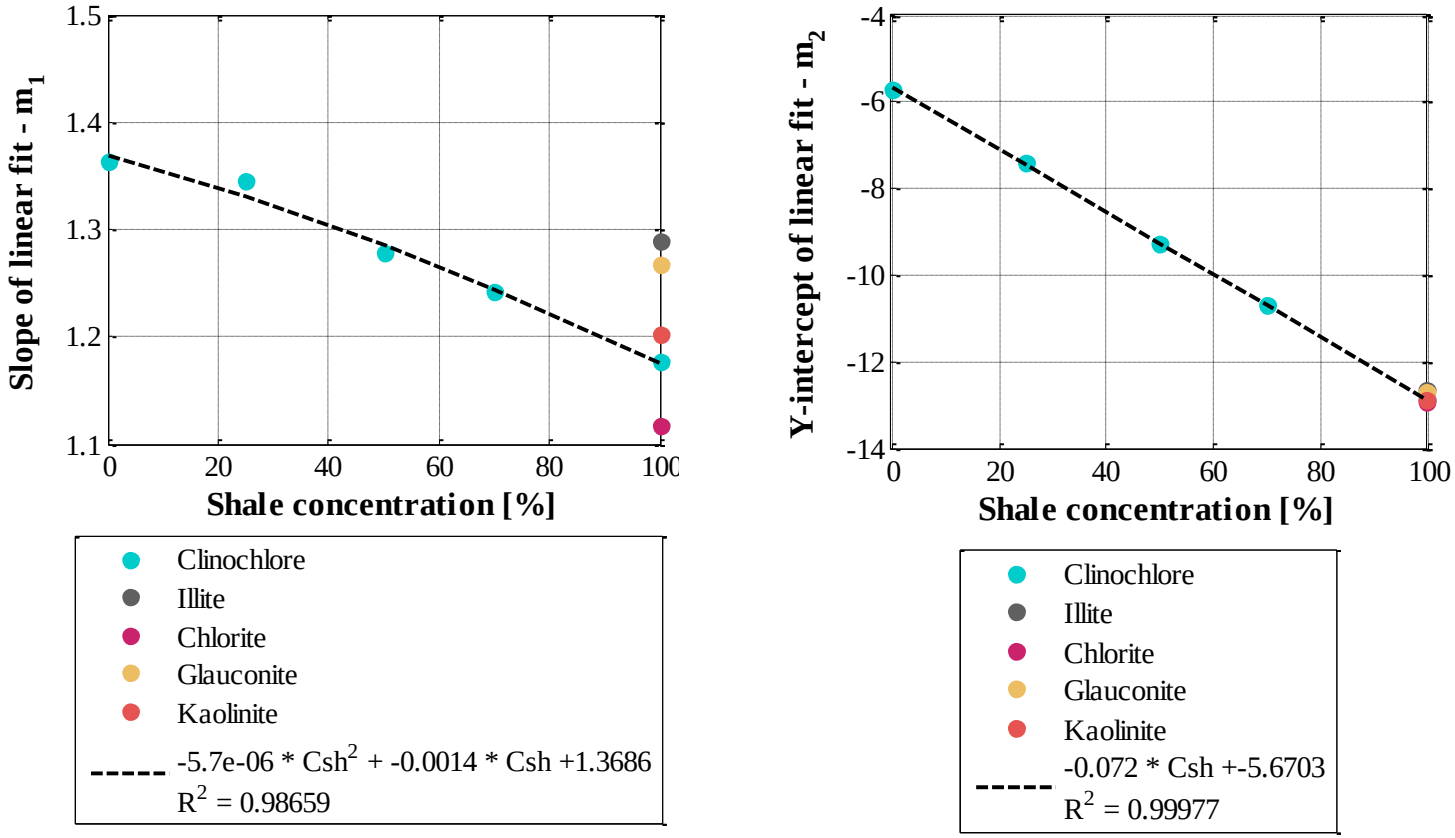

Figure 4.3. Linear equation for the linear fit dependence on C_{sh}. **Left** - Dependence of the slope of the linear fit. **Right** - Dependence of the Y-intercept of the linear fit

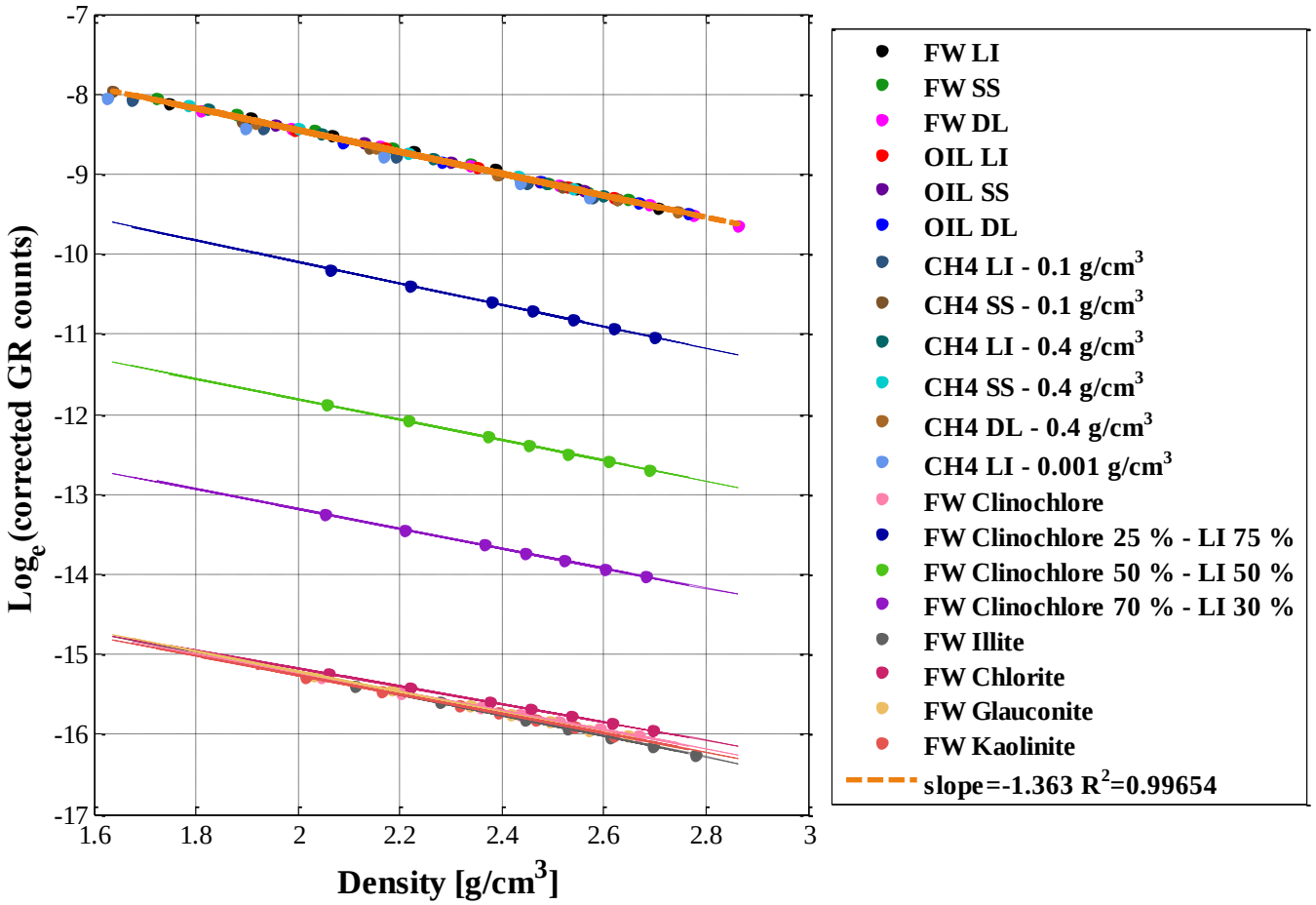

Figure 4.4: Results of inversion performed for clean formations in fresh water, oil and gas. Showing corrected gamma ray counts plotted against density.

Chapter 5: Density Limitations, Environmental Effects and, Depth of Investigation

In this chapter, we study the acceptable range of formations for the sourceless density measurement. We also study environmental effects and resulting limitations on standoff. Finally, we compare the depth of investigation of Neutron-Gamma density to that of Gamma-Gamma density.

5.1 Limitations in Density and Removal Cross Section

Neutron-Gamma density counts are attenuated by high densities during gamma ray transport and by the fast neutron removal cross section during fast neutron transport. The combination of both effect leads to poor statistics at the detectors. **Figure 5.1** shows that the product of density and removal cross section can be used to predict particle attenuation in different lithologies. The product of density and removal cross section is a quick technique to assess whether a certain formation yield poor statistics. In general, shale with high hydrogen content and high density yield the lowest counts. Higher hydrogen content results in decreased gamma ray production while higher density increases the likelihood that gamma rays undergo Compton scattering.

The real-time interpretation algorithm does not accurately estimate higher densities (densities greater than 2.89 g/cm^3) as illustrated by **figure 5.2**.

5.2 Environmental Effects

We study the environmental effects on the measurements. In **figure 5.3**, we investigate the influence of increasing standoff for different borehole sizes. The measurement of density is increasingly affected by the density of the mud when standoff

increases. Therefore, standoff is particularly significant in the presence of light mud because the density contrast with formation density is more important.

We recommend that the standoff be kept under 0.25 inch for a reliable Neutron-Gamma density measurement in light mud.

In **figure 5.4**, we study the influence of mud salinity and borehole size on the density measurement. Increased mud salinity has little to no influence on the density measurement. Similarly, increased borehole size with no standoff has little influence. A correction of 0.05 g/cm^3 would be required in a 10 inch borehole.

5.3 DEPTH OF INVESTIGATION

We compute the depth of investigation of Neutron-Gamma density and Gamma-Gamma density using the radial geometrical factor of the flux sensitivity functions of each measurement.

The Neutron-Gamma density source is located directly inside the formation. Therefore, the depth of investigation of Neutron-Gamma density (around 22 cm) is more than twice the depth of investigation of Gamma-Gamma density (**figure 5.5**).

The depth of investigation of Neutron-Gamma density is almost independent of changes in porosity, lithology and fluids (**figure 5.6**).

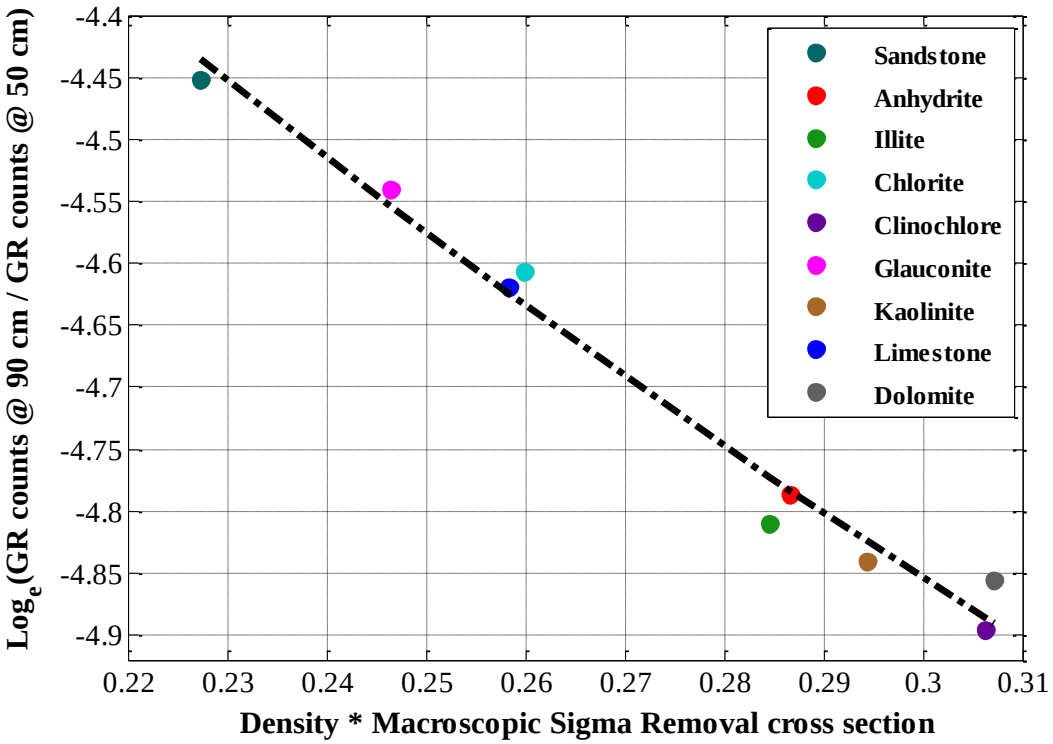

Figure 5.1: Attenuation capacity of different lithologies on Neutron-Gamma density counts.

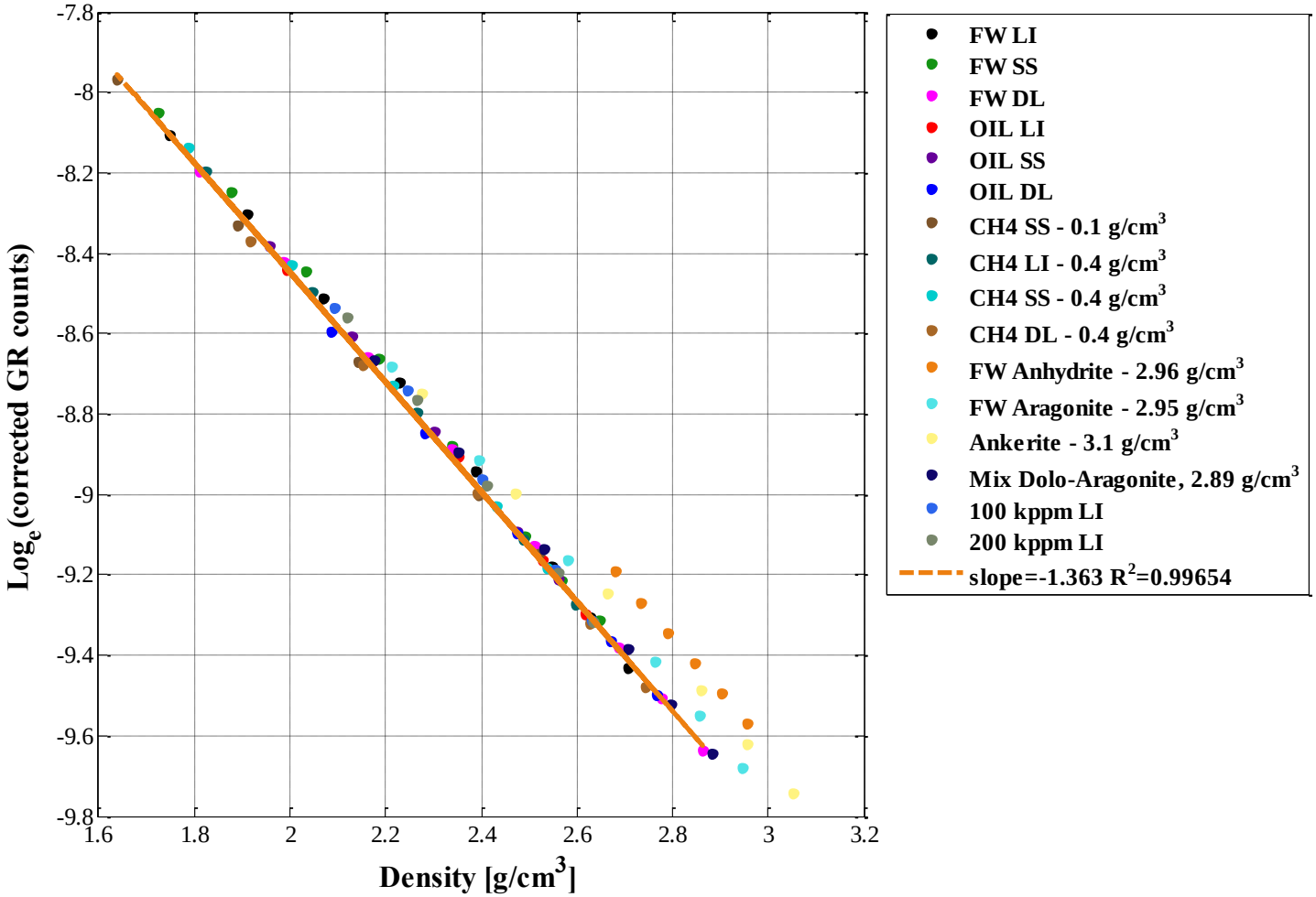

Figure 5.2: Inversion algorithm results for formations with densities higher than 2.89 g/cm^3.

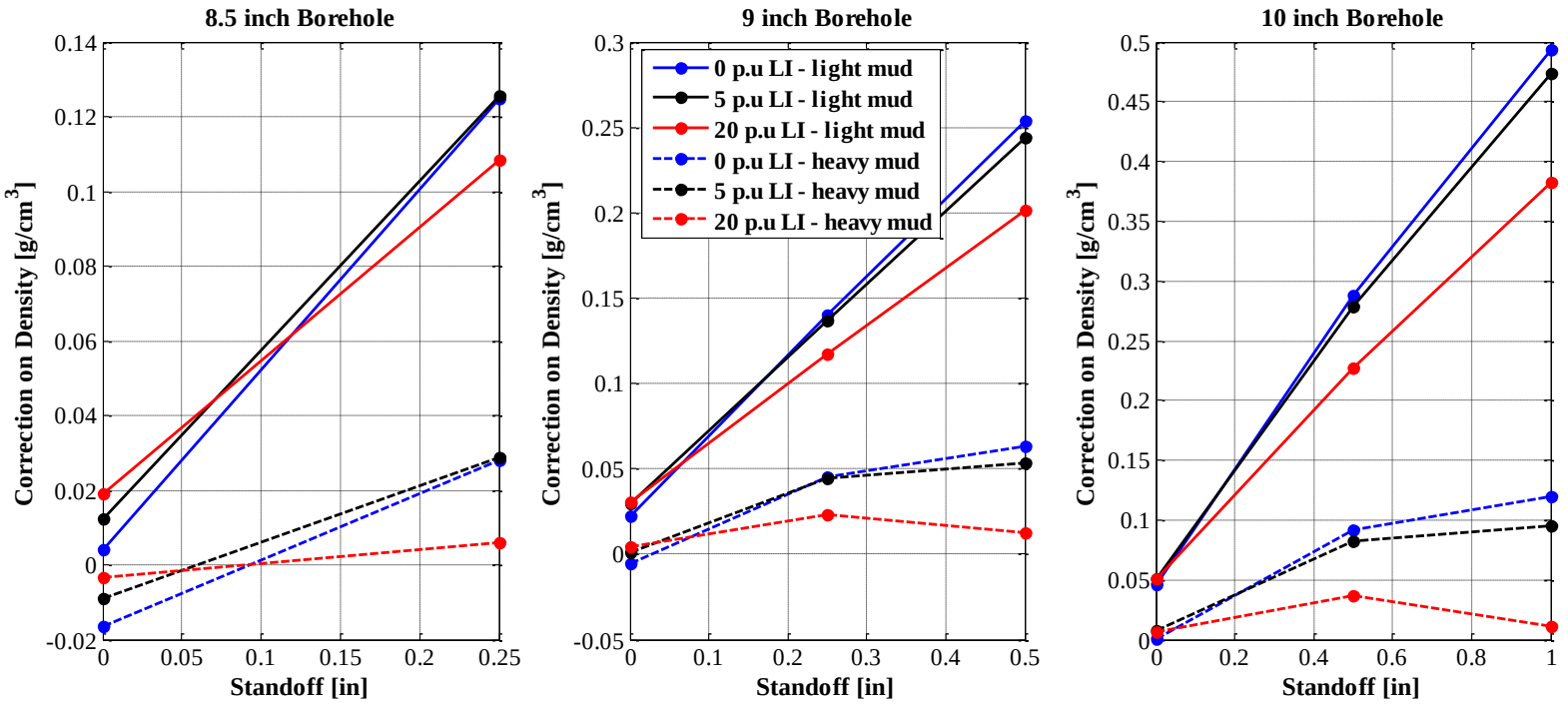

Figure 5.3: Correction on density in g/cm^3 versus increasing standoff for 8.5 in (**left**), 9 in (**center**), and 10 in (**right**) boreholes in limestone.

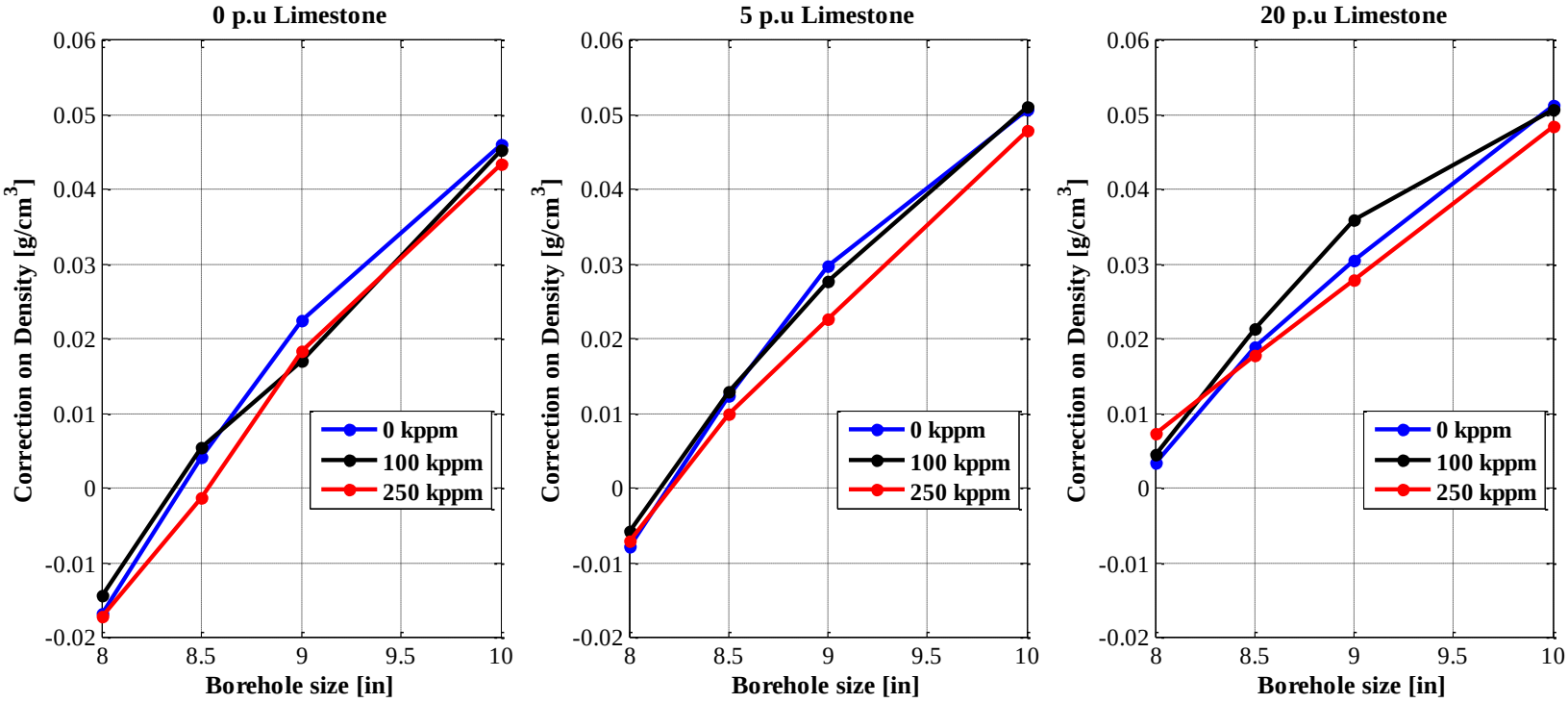

Figure 5.4: Correction on density in g/cm^3 versus borehole size (no standoff) for different mud salinities in a 0 p.u (**left**), 5 p.u (**center**), and 20 p.u (**right**) Limestone.

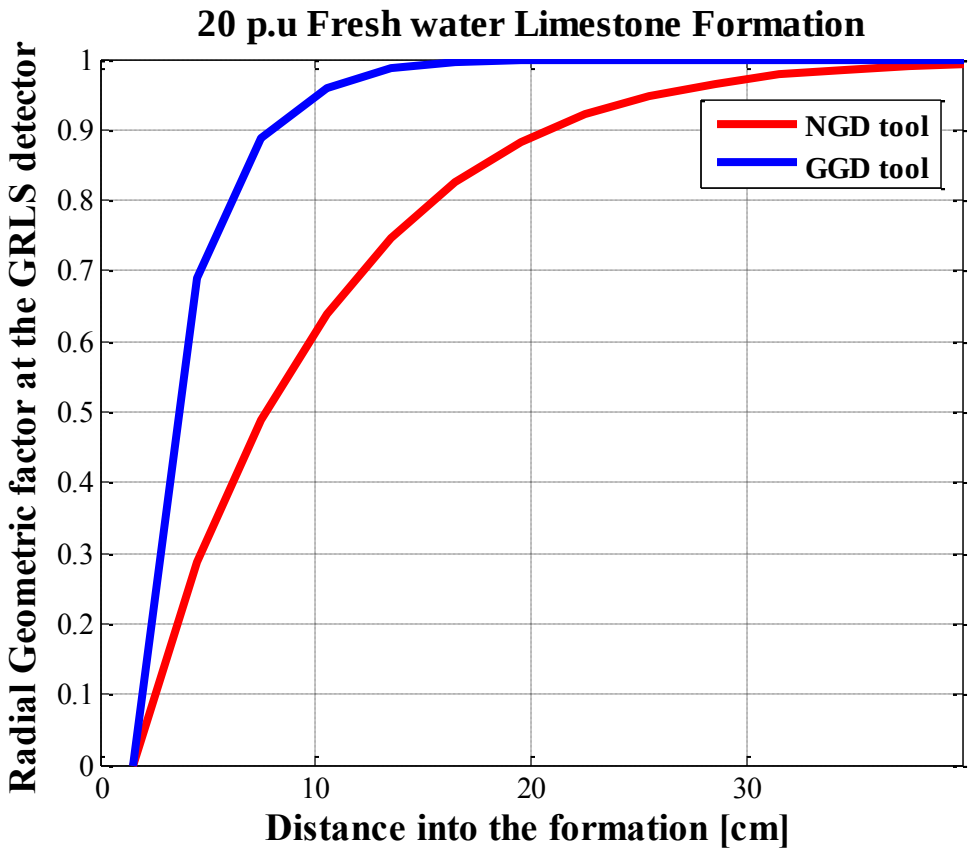

Figure 5.5: Comparison of the depth of investigation of Neutron-Gamma density and Gamma-Gamma density measurements.

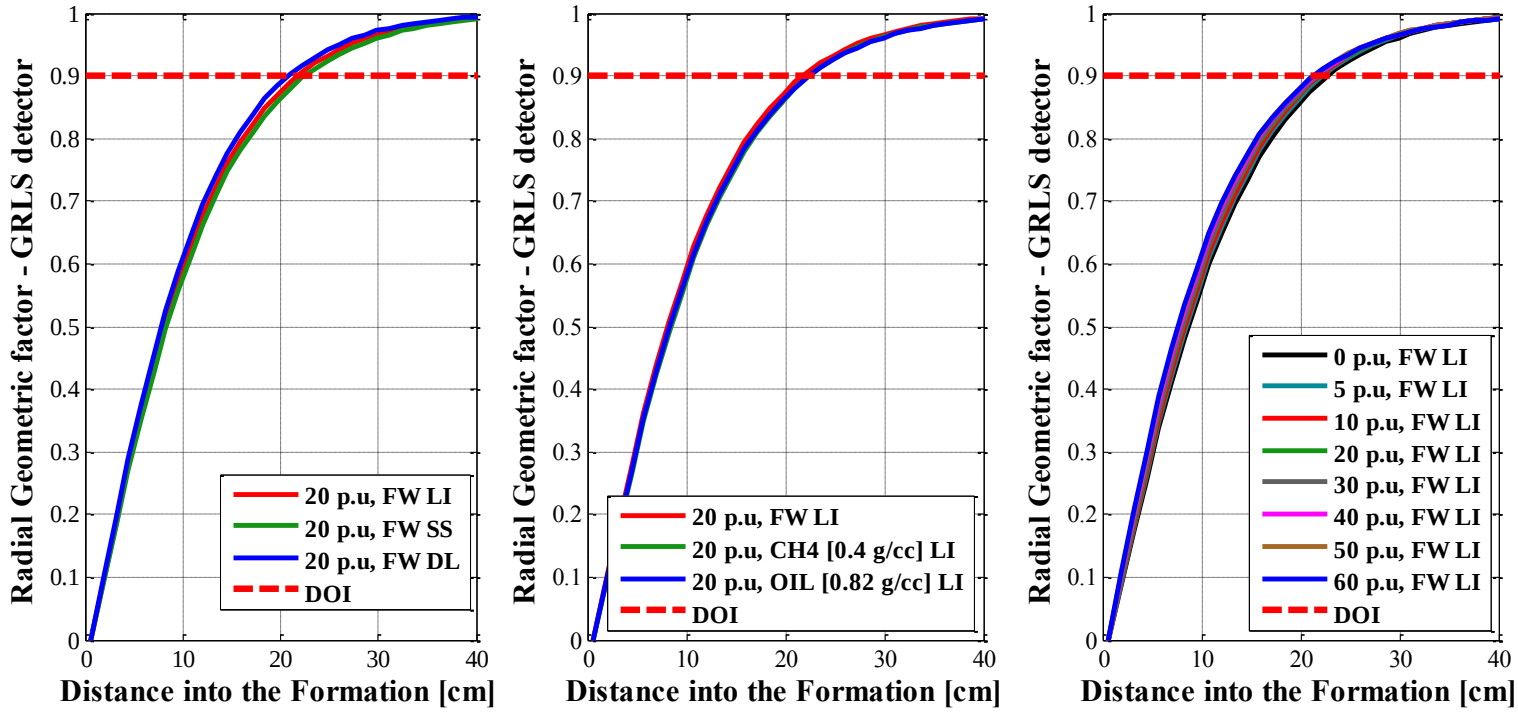

Figure 5.6: Depth of investigation of Neutron-Gamma density for different lithologies (**left**), formation fluids (**center**), and porosities (**right**).

Chapter 6: Conclusions

This work studies the feasibility and limitations for a sourceless measurement of density. The objective is to assess the possibility for replacing the traditional Gamma-Gamma density measurement with a radioisotope-free alternative.

Studying the physics of Neutron-Gamma density is essential to understand the impact of the different nuclear interactions on the counts. The measurement relies on counts generated during the burst of the pulsed neutron generator in order to limit neutron diffusion in the formation and therefore limit variations in the neutron-induced gamma ray source.

The neutron-induced gamma ray source remains influenced by formation changes and therefore the counts are affected by more than just formation density. We designed a synthetic tool in MCNP and optimized source – detector spacing towards optimal accuracy. We develop a real-time interpretation algorithm in order to correct for the influence of fast neutron transport and linearize tool response with respect to formation density. The density accuracy is 0.019 g/cm^3 in clean formations and 0.034 g/cm^3 in shale and shaly formations. However, the interpretation algorithm does not accurately estimate higher densities (densities greater than 2.89 g/cm^3).

We study the depth of investigation of the measurement which is more than twice the depth of investigation of Gamma-Gamma density and almost insensitive to changes in formations porosity, fluid and, lithology. The measurement is affected by environmental effects and particularly standoff. Standoff should be kept to a maximum of 0.25 inch in case of light mud.

Future work will be extended to a PhD dissertation. The tool design will be improved to further decrease the dependence of the measurement to lithology and the limitations in formation density. The real-time algorithm will be reviewed to increase measurement accuracy. We will develop fast forward modeling for enhanced interpretation in complex 3D geometries and in situations where standoff is affecting the measurement.

List of Symbols

C_{sh}	Shale concentration.
DL	Dolomite.
E	Particle energy.
Fast_N	Fast Neutron detector.
FSF	Flux sensitivity function.
FW	Fresh Water.
GGD	Gamma-Gamma density.
GR	Gamma ray.
GRLS	Gamma ray Long Space detector.
GRSS	Gamma ray Short Space detector.
LI	Limestone.
LWD	Logging while drilling.
MCNP	Monte Carlo N-Particle code.
NGD	Neutron-Gamma density.
p.u	Porosity unit.
r	Position vector.
S	Particle source (particles/cm^3-s-eV-ster).
SS	Sandstone.
t	Time.
v	Particle velocity.
ρ	Density (g/cm3).
Σ_s	Macroscopic scattering cross section (cm2/cm3).

Σ_t	Macroscopic total interaction cross section (cm2/cm3).
ψ	Angular flux (particles/cm2-s-eV-ster).
$\boldsymbol{\Omega}$	Angular direction (ster).

References

Aster, R. C., Borchers, B., and Thurber, C. H., 2005, Parameter estimation and inverse problems: Elsevier.

Booth, T. E., and Hendricks, J.S., 1984, Importance estimation in forward Monte Carlo calculations: Nuclear Technology / Fusion, vol. 5, pp. 90-100.

Bertozzi, W., Ellis, D.V., and Wahl, J.S., 1981, The physical foundation of formation lithology logging with gamma rays: Geophysics, 46 (10): pp. 1439-1455, October.

Case, C., Watson, C. C., and Lawrence, R., 1994, Sensitivity function technique for modeling nuclear tools: United Sates Patent 5,334,833.

Couët, B., and Watson, C. C., 1993, Monte Carlo differential neutron sensitivity calculations for nuclear well-logging: IEEE Transactions on Nuclear Science, vol. 40, no. 4, pp. 928-932.

Evans, M., Allioli, F., Cretoiu, V., Haranger, F., Laporte, N., Mauborgne, M., Nicoletti, L., Reichel, N. J., Stoller, C., Tarrius, M., Griffiths, R. J., 2012, Sourceless Neutron-Gamma Density (SNGD): A radioisotope-free bulk density measurement: physics principles, environmental effects, and applications: Society of Petroleum Engineers Annual Technical Conference and Exhibition, SPE-159334-MS.

Goorley T., 2014, MCNP6.1.1-Beta Release Notes, LA-UR-14-24680.

Lewis E. E., Miller W. F., 1938, Computational methods of neutron transport: John Wiley and Sons, Inc., New York, NY.

Mendoza, A., Torres-Verdín, C., and Preeg, W.E., 2010, Linear iterative refinement method for the rapid simulation of borehole nuclear measurements, Part I – Vertical wells: Geophysics, 75 (1): E9 – E29, January-February.

Mendoza, A., Torres-Verdín, C., and Preeg, W.E., 2010b, Linear iterative refinement method for the rapid simulation of borehole nuclear measurements, Part 2 – High-angle and horizontal wells: Geophysics, 75(2): E79-E90, March-April.

Mendoza, A., Torres-Verdín, C., and Preeg, W.E., 2007, Rapid simulation of borehole nuclear measurements with approximate spatial flux-scattering functions: Paper O, 48th SPWLA Symposium, June 3-6, Austin, Texas.

Reichel, N., Evans, M., Allioli, F., Mauborgne, M.-L., Nicoletti, L., Haranger, F., Laporte, N., Stoller, C., Cretoiu, V., El Hehiawy, E., Rabrei, R., 2012, Neutron-Gamma Density (NGD): principles, field test results and log quality control of a radioisotope-free bulk density measurement. 53rd SPWLA Symposium, June 16-20, Cartagena, Colombia.

Reichel, N. J., Prabawa, H., Mpanzu, A., and Crowe, J., 2011, Compensated neutron-gamma density for formation evaluation, continuing field tests demonstrate improvements and new features, Annual Conference and Exhibition, Society of Petroleum Engineers , 23-26 May, Vienna, Austria.

Tittman, J. and Wahl, J. S., 1965, The physical foundations of formation density logging (Gamma-Gamma), Geophysics, 30(2), 284-294.

Tittle, C.W., 1961, Theory of neutron logging: Geophysics, 26 (1): pp. 27-39, February.

Wahl, J. S., Tittman, J., & Johnstone, C. W., 1964, The dual spacing formation density log, Society of Petroleum Engineers, Journal of Petroleum Technology, 16(12).

Watson, C.C., 1984, Monte Carlo computation of differential sensitivity functions: Transactions of American Nuclear Society, 46, pp. 655.

Watson, C.C., 1992, A spatial sensitivity analysis technique for neutron and gamma ray measurements: Transactions of American Nuclear Society, 65, Suppl. 1, pp. 3.

Weller, G., Griffiths, R., Stoller, C., & Allioli, F., 2005, A new integrated LWD platform brings next-generation formation evaluation services. Transactions of the Society of Petrophysicists and Well-Log Analysts, 46th Annual Logging Symposium.